

## Determining the Material and Physical Properties of Alloy $\text{La}_{0.85}\text{Ce}_{0.15}\text{Ni}_5$ Used in Hydrogen Storage

N. Jasminská,<sup>a,1</sup> T. Brestovič,<sup>a,2</sup> M. Lázár,<sup>a,3</sup> K. Saksl,<sup>b,4</sup> K. Šulová,<sup>b,5</sup> M. Čarnogurská,<sup>a,6</sup> and L. Bednárová<sup>a,7</sup>

<sup>a</sup> Technical University in Košice, Košice, Slovakia

<sup>b</sup> Slovak Academy of Sciences in Košice, Košice, Slovakia

<sup>1</sup> natalia.jasminska@tuke.sk

<sup>2</sup> tomas.brestovic@tuke.sk

<sup>3</sup> marian.lazar@tuke.sk

<sup>4</sup> ksaksl@imr.saske.sk

<sup>5</sup> ksulova@imr.saske.sk

<sup>6</sup> maria.carnogurska@tuke.sk

<sup>7</sup> lubica.bednarova@tuke.sk

The article addresses the determination of the physical and material properties of the alloy  $\text{La}_{0.85}\text{Ce}_{0.15}\text{Ni}_5$  with a crystalline structure. The properties of the microstructure of the alloy were determined using a scanning electron microscope. The chemical composition was evaluated by energy-dispersive X-ray spectroscopy. An X-ray diffractometer was used to determine the phase composition of the alloy. Next, the alloy sample was subjected to measurements of hardness, thermal conductivity and heat capacity. The storage capacity of hydrogen in the alloy was determined using the pressure concentration isotherms method of measuring. For comparison, the storage capacity was also measured in the amorphous structure of the alloy formed by the melt spinning method.

**Keywords:** metalhydrid, hydrogen, hydrogen storage, material properties, alloy.

**Introduction.** Storing hydrogen in the form of intermetallic metal hydrides was intensively studied in the beginning with the alloys  $\text{LaNi}_5$  and  $\text{FeTi}$ , with positive results enabling extension of the capabilities of metal hydride storage for industry [1, 2]. For influencing the equilibrium pressure of hydrogen absorption in the hexagonal lattice some of the La atoms were replaced with Ce, thereby achieving maximum internal and cyclic stability of the absorption and desorption of hydrogen [3, 4]. To obtain the complex properties of the selected alloy  $\text{La}_{0.85}\text{Ce}_{0.15}\text{Ni}_5$  a series of physical measurements were carried out. The knowledge gained is helpful not only for the proper formation of structures necessary for the absorption of hydrogen, but also for energy optimization of metal hydride containers [5, 6]. Given that increase in kinetic desorption of hydrogen requires the use of finer fractions of the alloy; it is necessary to know the thermal conductivity of alloy so that with refining, the fraction becomes smaller.

The examined alloy of type AB5 with composition  $\text{La}_{0.85}\text{Ce}_{0.15}\text{Ni}_5$  was manufactured by Labtech Ltd in Sofia, Bulgaria. Given that no information was available on the commercially prepared alloy, measurements were subsequently made of the material's properties, thermal conductivity and capacity of the Institute of Materials Research of the Slovak Academy of Sciences in Košice.

Upon this alloy, structural, phase and chemical analysis was conducted using the methods of light microscopy (LM), scanning electron microscopy (SEM), energy-dispersive spectroscopy (EDS), and X-ray diffraction (XRD). Equally, hardness measurements were

taken on the alloy using the method of Vickers tip microindentation under a load of 300 gf (2.942 N).

For effective absorption storage of hydrogen, the most suitable is a crystalline structure and a finer fraction of the intermetallic alloy [7]. For the proper design of the heat exchanger of the cooling device, which is used for cooling the alloy during absorption, it is necessary to know the heat capacity and thermal conductivity of the alloy [8, 9].

**Microstructure of  $\text{La}_{0.85}\text{Ce}_{0.15}\text{Ni}_5$  Alloy.** To observe the microstructure of the alloy  $\text{La}_{0.85}\text{Ce}_{0.15}\text{Ni}_5$  an Olympus GX 71 light microscope was used. The actual observation of the surface of the samples was carried out in modes of reflected unpolarized light, polarized light, as well as in phase contrast mode (Nomarski differential interference contrast). The metallographic sample of the alloy was prepared as follows:

(i) the sample was moulded into a Struers POLYFAST conductive resin at 180°C and a pressure of 18 MPa in a Buehler SimpliMet 3000 machine. The process of pressing the resin into the sample consisted of melting and cooling at a time interval of 30 min;

(ii) sanding was performed using P600 sandpaper, and was carried out at a constant pressure of 9 N for a time interval of 120 s. Subsequently, P1200 and P2500 sandpaper were used again at constant pressure of 9 N for a time interval of 120 s;

(iii) polishing was carried out using a polishing cloth without water for 60 s followed by the addition of polishing emulsion 50 nm (120 s), 20 nm (120 s). The sample was finished by polishing with intensive addition of water (60 s).

To highlight the alloy microstructure of  $\text{La}_{0.85}\text{Ce}_{0.15}\text{Ni}_5$  three kinds of chemical etchants were used that are recommended for Ni alloys:

(1). Etching using etchant No. 52. Composition of etchant: 60 ml glycerol, 50 ml of HCl, and 10 ml of  $\text{HNO}_3$ . With a time interval of 10 s no change in the surface of the alloy was observed. Repeated etching of the material for 50 s without prior rubbing and polishing took place without significant change of enhancement of the microstructure.

(2). Etching using etchant No. 48. Composition of etchant: 5 g  $\text{FeCl}_3$ , 2 ml HCl, and 99 ml ethanol.

(3). Etching using Kroll's solution. Composition of etchant: 100 ml  $\text{H}_2\text{O}$ , 6 ml  $\text{HNO}_3$ , and 3 ml HF. With a time interval of 10 s there was a change in the surface of the alloy in the form of etch patterns as a result of etching through.

From the above it can be concluded that conventional methods of sample preparation that are applied to nickel and supernickel alloys do not result in etching of the grain boundaries, i.e., to the highlighting of the polycrystalline structure of the alloy  $\text{La}_{0.85}\text{Ce}_{0.15}\text{Ni}_5$ .

The surfaces shown in Figs. 1–3 were prepared by grinding, polishing, but were not chemically etched. As will be shown below, the alloy  $\text{La}_{0.85}\text{Ce}_{0.15}\text{Ni}_5$  consists of only one intermetallic phase, specifically hexagonal  $\text{La}(\text{Ce})\text{Ni}_5$ , the highlighting (etching of grain boundaries) of which is difficult. When viewing the surface alloys modes of observation were used with collection of secondary electrons (TOPO viewing mode) as well as backscattered electrons (COMPO mode).

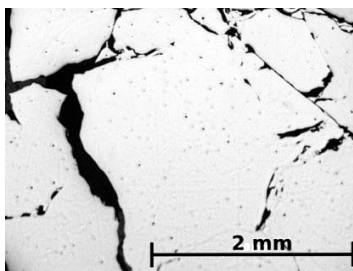


Fig. 1. Microstructure of alloy  $\text{La}_{0.85}\text{Ce}_{0.15}\text{Ni}_5$  viewed using light microscopy. Magnification  $\times 20$ .

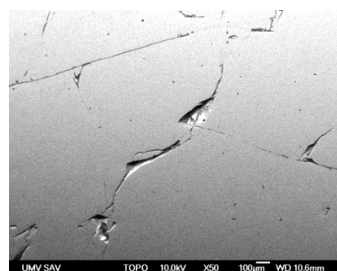


Fig. 2. Microstructure of alloy  $\text{La}_{0.85}\text{Ce}_{0.15}\text{Ni}_5$  viewed in mode with collection of secondary electrons (TOPO). Magnification  $\times 50$ .

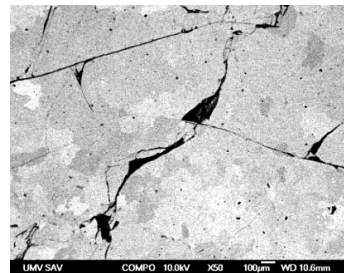


Fig. 3. Microstructure of alloy  $\text{La}_{0.85}\text{Ce}_{0.15}\text{Ni}_5$  view in mode with collection of back scattered electrons (COMPO). Magnification  $\times 50$ .

**Chemical Composition of  $\text{La}_{0.85}\text{Ce}_{0.15}\text{Ni}_5$  Alloy.** To view the microstructure and chemical analysis, we used a JEOL JSM-7000F multi-functional high-resolution scanning electron microscope with a THERMAL FEG field-emission gun. The microscope allows the maximum possible magnification,  $\times 100,000$  and the maximum resolution is 1.2 nm. The microscope also includes an EDX detector, which enables the realization of elemental chemical composition (from boron) in submicron volumes.

The chemical composition of  $\text{La}_{0.85}\text{Ce}_{0.15}\text{Ni}_5$  alloy was evaluated using the method of energy-dispersive X-ray spectroscopy (EDS). The EDS detector device is part of the kit of the JEOL JSM 7000F scanning electron microscope. The area from which the signal was obtained by the EDS is shown in the pink rectangle in Fig. 4. The resolution of the spectrum 123 eV (FWHM) as measured on the  $\text{Ni}-\text{K}\alpha$  emission lines. The X-ray-emission spectrum (Fig. 5) was obtained by scanning the electron beam over the surface of the sample on the surface of approx.  $5 \text{ mm}^2$ .

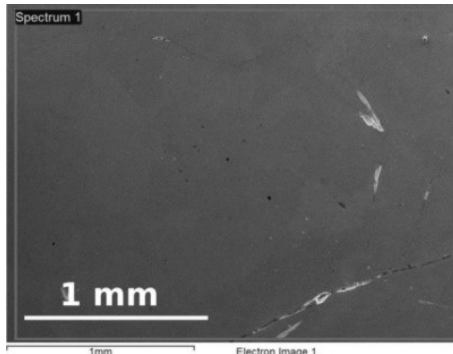


Fig. 4

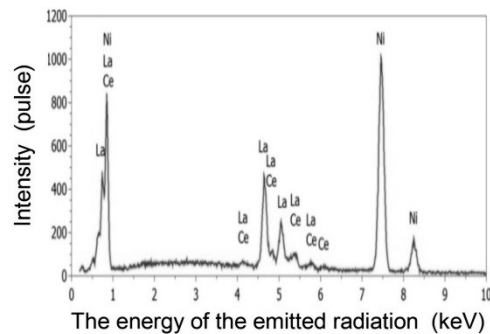


Fig. 5

Fig. 4. EDS chemical analysis of alloy  $\text{La}_{0.85}\text{Ce}_{0.15}\text{Ni}_5$  ground, polished, not chemically etched surface of the  $\text{La}_{0.85}\text{Ce}_{0.15}\text{Ni}_5$  alloy obtained by recording secondary electrons at a magnification of  $\times 50$ .

Fig. 5. EDS chemical analysis of alloy  $\text{La}_{0.85}\text{Ce}_{0.15}\text{Ni}_5$  energy-dispersive spectrum emitted X-ray radiation obtained by scanning the surface with an approx  $5 \text{ mm}^2$  electron beam accelerated to 20 keV.

From the EDX spectrum obtained, semi-quantitative analysis (INCA Oxford Instruments software) was used to obtain the elemental composition of the sample quantitatively (Table 1).

By comparing the chemical composition determined by measuring with that stated by the manufacturer it is possible to state very good conformance. Moreover, the presence of any other elements (impurities) was not confirmed.

Table 1

**Chemical Composition of La<sub>0.85</sub>Ce<sub>0.15</sub>Ni<sub>5</sub> Alloy Obtained by Semi-Quantitative Analysis of Measured EDX Spectrum**

Element	Mas.%	At.%
Ni K	66.54	82.50
La L	27.91	14.62
Ce L	5.55	2.88
Total	100.00	100.00

**Phase Composition of La<sub>0.85</sub>Ce<sub>0.15</sub>Ni<sub>5</sub> Alloy.** To determine the phase composition of the La<sub>0.85</sub>Ce<sub>0.15</sub>Ni<sub>5</sub> alloy a Philips X'Pert Pro X-ray diffractometer was used. With X-ray diffraction measurement Cu anode (wavelength  $K\alpha_1 = 0.154056$  nm,  $K\alpha_2 = 0.154439$  nm, and ratio of the intensities  $IK\alpha_2/IK\alpha_1 = 0.5$ ) radiation was used, the scope of measurement of  $2\Theta$  was 20–150° with a step of 0.01671°, the measuring time at each step was 10 s. Prior to measurement the sample was crushed to a powder in a vibrating mill. The powder was poured into the sample holder to ensure the random orientation of crystallites of the measured the alloy.

The phase composition of La<sub>0.85</sub>Ce<sub>0.15</sub>Ni<sub>5</sub> alloy was determined by X-ray diffraction. Figure 6 shows the output measurements (symbol ○), together with a more accurate model of the hexagonal phase La(Ce)Ni<sub>5</sub>. As can be seen, the degree of conformity of model and measurement expressed by parameter Rwp (relative error of approximation) is very good, based on which it can be concluded that the alloy La<sub>0.85</sub>Ce<sub>0.15</sub>Ni<sub>5</sub> consists solely of a single phase.

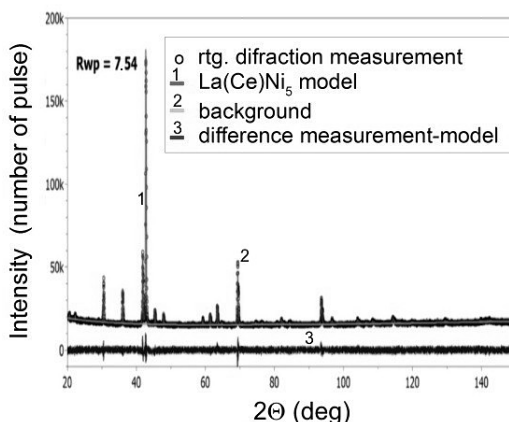


Fig. 6. Measured X-ray diffraction (○) display together with the model phase of La(Ce)Ni<sub>5</sub>, the defined background measurement and the differential curve between measurement and model.

Phase La(Ce)Ni<sub>5</sub> crystallizes in a hexagonal system, it has spatial group P6/mmm (191) with a size of lattice parameters  $a = 0.498(4)$  nm and  $c = 0.399(4)$  nm. The model was made more detailed using the Rietveld refinement on experimental data obtained in the program implemented in the PowderCell program.

The size of crystallites in this phase is approximately 200 nm and the size of microdeformations is on the level of  $0.4 \cdot 10^{-4}\%$ , the values of these parameters were determined using the Williamson–Hall method. The atomic model of phases of La(Ce)Ni<sub>5</sub> is shown in Fig. 7.

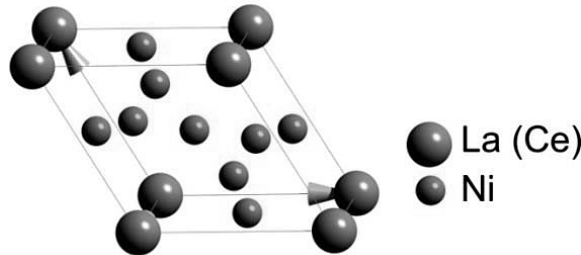


Fig. 7. Atom model of basic cell of crystalline phase of  $\text{La}(\text{Ce})\text{Ni}_5$ .

The special position of lanthanum in the cell is shared by 85% atoms of La and 15% atoms of Ce.

**Measuring the Hardness of  $\text{La}_{0.85}\text{Ce}_{0.15}\text{Ni}_5$  Alloy.** To measure the hardness of alloy, a Wilson Tukon 1102 Knoop/Vickers microhardness tester was used, operating in the range 10–1000 gf (gram force). To determine the hardness of  $\text{La}_{0.85}\text{Ce}_{0.15}\text{Ni}_5$  alloy the Vickers tip test was used with a force of 300 gf (2.942 N), whereby the time of load during indentation was 5 s. A total of 10 measurements were performed, the mean and standard deviation of hardness HV0.3 was determined from 8 measurements after removal of the extreme values.

The mean hardness of the  $\text{La}_{0.85}\text{Ce}_{0.15}\text{Ni}_5$  alloy was determined as  $676 \pm 17$  HV0.3 using the arithmetical mean of the 8 measurements of the Vickers indentation test into the sample with the application of a load force of 2.942 N (300 gf). The hardness of the single-phase  $\text{La}_{0.85}\text{Ce}_{0.15}\text{Ni}_5$  alloy consisting exclusively of a hexagonal intermetallic  $\text{La}(\text{Ce})\text{Ni}_5$  phase is comparable to the hardness of TiNi intermetallic phases or AISI 440C, AISI 52100 stainless steel.

**Thermal Conductivity and Capacity of  $\text{La}_{0.85}\text{Ce}_{0.15}\text{Ni}_5$  Alloy.** The apparatus for measuring thermal conductivity using the flash method was used to measure thermal diffusivity with the Cape Lehman model with pulse correction. Specific heat capacity was determined using the reference standard for stainless steel 310. Thermal conductivity was calculated from thermal diffusivity, density and specific heat capacity using Eq. (1),

$$a = \frac{\lambda}{cp} \quad (\text{m}^2/\text{s}), \quad (1)$$

where  $a$  is the thermal diffusivity ( $\text{m}^2/\text{s}$ ),  $\lambda$  is the thermal conductivity [ $\text{W}/(\text{m} \cdot \text{K})$ ],  $c$  is the specific heat capacity [ $\text{J}/(\text{kg} \cdot \text{K})$ ], and  $\rho$  is the density ( $\text{kg}/\text{m}^3$ ), see Table 2.

**Measuring the Storage Capacity of the Alloy during Absorption of Hydrogen.** Determining the storage capacity of the alloy in storing hydrogen in the form of a metal hydride was performed by volumetric methods [10]. Two samples of the alloy with the same composition but different structures were used. Sample No. 1 was made by slow cooling, to obtain crystal structure, whereby the material properties were as described in the previous chapters of this article. Sample No. 2 was produced by the melt spinning method, which guarantees an amorphous structure.

Initially, both samples were activated in the same conditions in a hydrogen atmosphere (99.999%  $\text{H}_2$ ), the pressure and temperature varied according to Fig. 8 to ensure the removal of residual gases and oxides.

The absorption capacity of the  $\text{La}_{0.85}\text{Ce}_{0.15}\text{Ni}_5$  alloy with an amorphous structure was reached only after its activation. During activation the temperature sharply varied between 0 and 100°C. In the first part of activation the pressure varied between a vacuum and 1 MPa, and in the last phase of activation between a vacuum and 5 MPa.

Table 2

**Thermal Conductivity, Thermal Diffusivity Specific Heat Capacity of the Sample  
of  $\text{La}_{0.85}\text{Ce}_{0.15}\text{Ni}_5$**

Measurement No.	Thermal diffusivity (mm <sup>2</sup> /s)	Thermal conductivity [W/(m · K)]	Specific heat capacity [kJ/(kg · K)]
1	4.634	16.941	0.436
2	4.506	16.473	0.435
3	4.637	16.952	0.431
4	4.606	16.836	0.446
5	4.563	16.679	0.447
Average	4.589	16.776	0.439
Standard uncertainty	0.025	0.090	0.003
Relative uncertainty (%)	0.538	0.538	0.724

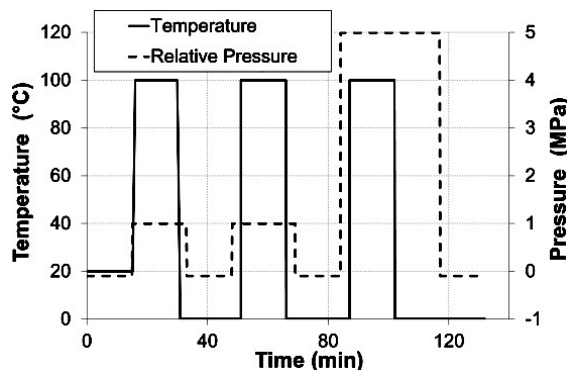


Fig. 8. Pressure and temperature during activation of the alloy.

The alloy with crystal structure demonstrated the ability to absorb hydrogen without activation. For the sake of comparability of measurement results, activation was performed on both samples under the same conditions. Already during activation, the sample was placed in a reaction vessel of a volume of 20 cm<sup>3</sup>. Sample No. 1 (crystal structure) had a mass of 72.87 g of a sample No. 2 (amorphous structure) had a mass of 60.27 g. The block circuit diagram for measurement of storage capacity of hydrogen absorption of the alloy is shown in Fig. 9.

The approach of indirect measurement of pressure concentration isotherms consists of the gradual discharge of the hydrogen in the measuring cylinder under isothermal reduction of pressure in the reaction vessel, in which there is a sample of the alloy. In measuring it is necessary to determine the mass of hydrogen stored with the empty reaction vessel without the alloy depending on the pressure of hydrogen under isothermal conditions. Comparison of the storage capacity of the empty reaction vessel and the reaction vessel with the alloy (Fig. 10) allows determination of the mass concentration of hydrogen stored (Fig. 11).

The mass concentration was determined using an indirect measuring method with subsequent calculation following the relationship:

$$c = \frac{m_s - m_v}{m_{MH}} \cdot 100\%, \quad (2)$$

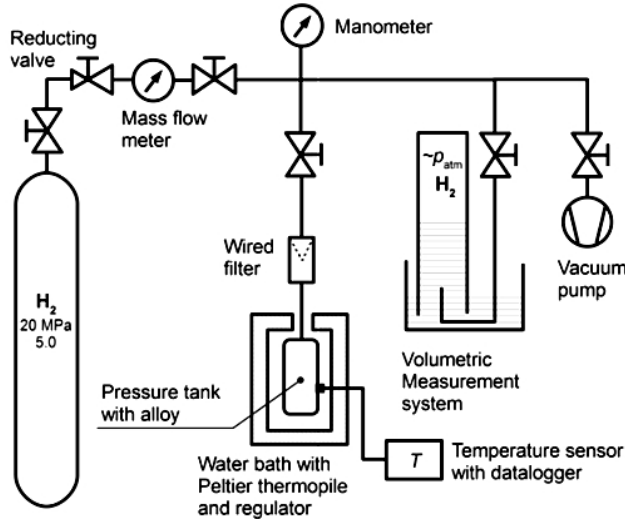


Fig. 9. Block diagram for the measurement of storage capacity of alloy.

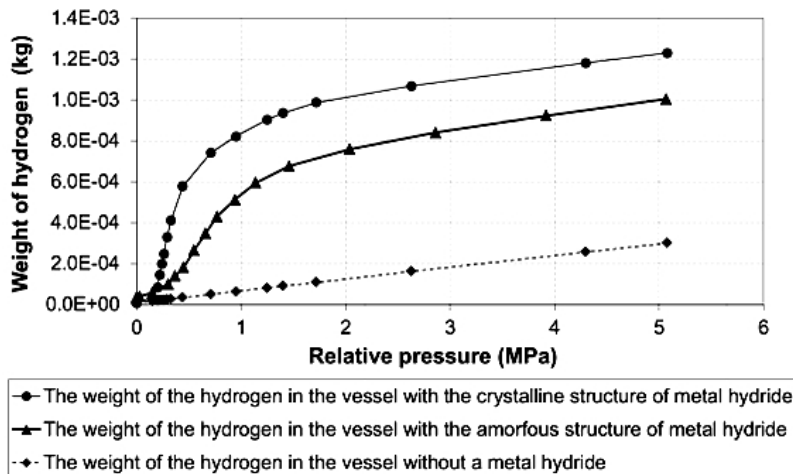


Fig. 10. Comparison of the amount of hydrogen stored in the empty container and when using samples with amorphous and crystalline structure.

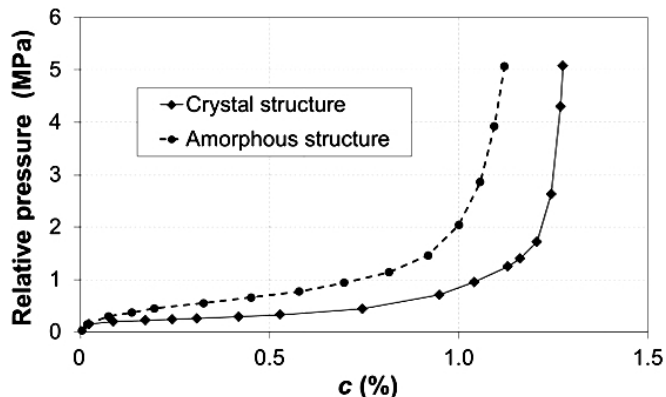


Fig. 11. Pressure concentration isotherms at a temperature of 20°C.

where  $c$  is the mass concentration of stored hydrogen (%),  $m_s$  is the mass of stored hydrogen in the container with alloy (kg),  $m_v$  is the mass of stored hydrogen in the container without alloy (kg), and  $m_{MH}$  is the mass of sample of alloy (kg).

In Fig. 11 there is comparison of the pressure concentration isotherms of the alloy with crystal and amorphous structure.

The mass concentration of crystalline  $\text{La}_{0.85}\text{Ce}_{0.15}\text{Ni}_5$  is 1.28 wt.% whereby the figure for the amorphous structure is 1.12 wt.%. The influence of the structure on the course of pressure concentration isotherms is visible also in the increase the equilibrium desorption pressure for an amorphous structure. The equilibrium pressure of the crystalline structure approximately 0.33 MPa, the alloy of amorphous structure has mean equilibrium pressure of 0.77 MPa.

**Conclusions.** From measurements of the microstructure it is shown that the  $\text{La}_{0.85}\text{Ce}_{0.15}\text{Ni}_5$  alloy consists of only one intermetallic phase, namely of hexagonal  $\text{La}(\text{Ce})\text{Ni}_5$ . The grain size of the crystalline  $\text{La}_{0.85}\text{Ce}_{0.15}\text{Ni}_5$  is in the range of  $100 \mu\text{m}$  to a few mm. The mean hardness of the alloy was determined to be  $676 \pm 17$  HV. The thermal conductivity was determined as  $16.776 \text{ W}/(\text{m}\cdot\text{K})$  and the specific heat capacity was  $439 \text{ J}/(\text{kg}\cdot\text{K})$ . These values are important in the design of thermal management of metal hydride containers. Subsequently, the storage capacity of hydrogen was measured in the alloy in the crystalline and amorphous structure of the sample. From the measured data it was shown that the crystalline structure of the alloy reduces the desorption pressure by more than half and slightly increases the mass concentration of hydrogen stored at 1.28 wt.%. In the case of 1 kg of alloy the container can store  $0.142 \text{ m}^3$  of hydrogen. With an amorphous structure the mass concentration of the hydrogen stored was 1.12 wt.%.

**Acknowledgments.** This paper was written with the financial support of the granting agency APPV within the project solution No. APVV-15-0202, of the granting agency VEGA within the project solution No. 1/0752/16 and of the granting agency KEGA within the project solution No. 005TUKE-4/2016.

1. M. Martin, C. Gommel, C. Borkhart, and E. Fromm, "Absorption and desorption kinetics of hydrogen storage alloys," *J. Alloy. Compd.*, **238**, Nos. 1–2, 193–201 (1996).
2. P. Tauš, M. Taušová, D. Šlosár, et al., "Optimization of energy consumption and cost effectiveness of modular buildings by using renewable energy sources," *Acta Montan. Slovaca*, **20**, No. 3, 200–208 (2015).
3. K. H. Buschow and H. H. Van Mal, "Phase relations and hydrogen absorption in the lanthanum-nickel system," *J. Less-Common Met.*, **29**, No. 2, 203–210 (1972).
4. H. Y. Cai, P. Millet, and P. Dantzer, "Intermetallic hydrides: (1) investigation of the rate of phase transformation," *J. Alloy. Compd.*, **231**, Nos. 1–2, 427–433 (1995).
5. P. D. Goodell and P. S. Rudman, "Hydriding and dehydriding rates of the  $\text{LaNi}_5\text{-H}$  system," *J. Less-Common Met.*, **89**, No. 1, 117–125 (1983).
6. N. Jasminská, T. Brestovič, and M. Lázár, *Výroba a Uskladnenie Vodika* [in Slovakian], TU, Košice (2015). ISBN 978-80-553-2378-7.
7. A. V. Klimyenko, J. Seuntjens, J. L. L. Miller, et al, "Structure of  $\text{LaNi}_{2.286}$  and the  $\text{La-Ni}$  system from  $\text{LaNi}_{1.75}$  to  $\text{LaNi}_{2.50}$ ," *J. Less-Common Met.*, **144**, No. 1, 133–141 (1988).
8. J. Kapischke and J. Hapke, "Measurement of the effective thermal-conductivity of a metal hydride bed with chemical-reaction," *Exp. Therm. Fluid Sci.*, **9**, No. 3, 337–344 (1994).

9. D. Ohlendorf and H. E. Flotow, “Heat-capacities and thermodynamic functions of LaNi<sub>5</sub>, LaNi<sub>5</sub>H<sub>0.36</sub> and LaNi<sub>5</sub>H<sub>6.39</sub> from 5 to 300 K,” *J. Less-Common Met.*, **73**, No. 1, 25–32 (1980).
10. N. Jasminská, T. Brestovič, and M. Čarnogurská, “Vodikove technologie na TUKE,” in: 32 Stretnutie Katedier Mechaniky Tekutin a Termomechaniky [in Slovakian], Edis, Žilina (2013), pp. 95–98, ISBN 978-80-554-0715-9.

Received 01. 09. 2017